

Addition of benzenethiol to terminal alkynes catalyzed by hydrotris(3,5-dimethylpyrazolyl)borate–Rh(III) bis(thiolate) complex: Mechanistic studies with characterization of the key intermediate

Yoshiyuki Misumi, Hidetake Seino, Yasushi Mizobe *

Institute of Industrial Science, the University of Tokyo, Tokyo, Japan

Received 4 January 2006; accepted 2 March 2006

Available online 9 March 2006

Abstract

The Rh(III)–thiolate complex $[\text{Tp}^*\text{Rh}(\text{SPh})_2(\text{MeCN})]$ (**2**; Tp^* = hydrotris(3,5-dimethylpyrazolyl)borate) readily undergoes substitution of MeCN by XyNC (Xy = 2,6-dimethylphenyl) to give the isocyanide complex $[\text{Tp}^*\text{Rh}(\text{SPh})_2(\text{XyNC})]$ (**3**), whereas reaction of **2** with terminal alkynes results in the formation of the rhodathiacyclobutene complex $[\text{Tp}^*\text{Rh}(\text{SPh})\{\eta^2\text{-CH=CR}(\text{SPh})\}]$ (**4**; R = aryl, alkyl). Molecular structures of **3** and **4** (R = CH_2Ph) have been determined by single crystal X-ray diffraction. Complex **2** as well as $[\text{Tp}^*\text{Rh}(\text{cyclooctene})(\text{MeCN})]$ have been found to catalyze regioselective addition of benzenethiol to terminal alkynes $\text{RC}\equiv\text{CH}$ at 50°C to give $\text{R}(\text{PhS})\text{C}=\text{CH}_2$ in moderate to high yields. The above products are selectively formed when $\text{R} = \text{CH}_2\text{Ph}$ and $n\text{-C}_6\text{H}_{13}$, while *cis*- $\text{RCH}=\text{CHSPh}$ and $\text{RC}(\text{SPh})_2\text{CH}_3$ are also obtained as by-products when $\text{R} = p\text{-MeOC}_6\text{H}_4$. Catalytic cycle involving **2** and **4** is proposed based on the mechanistic studies using NMR measurement.

© 2006 Elsevier B.V. All rights reserved.

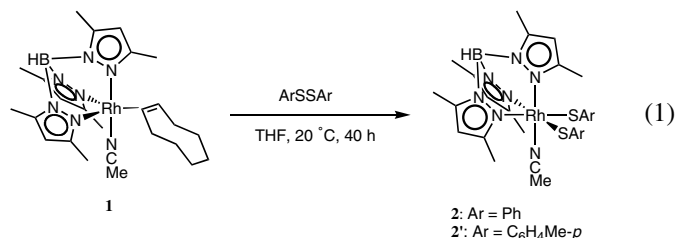
Keywords: Hydrotris(pyrazolyl)borate; Rhodium(III) thiolato complexes; Rhodathiacyclobutene; Hydrothiolation of alkyne

1. Introduction

Thiolate ligands are not only good electron-donors but also effective bridging ligands between two or more metal atoms to form multinuclear complexes [1–7]. Due to high affinity of sulfur atoms with transition metals, thiolate ligands in transition metal catalysts usually play an important role to maintain the coordination sphere around the metal center or multimetallic core [8–13]. On the other hand, thiolate complexes often become the key intermediates in metal-aided C–S bond forming reactions that proceed stoichiometrically [14,15] and catalytically [16–19].

In contrast to the rich chemistry of thiolate complexes containing cyclopentadienyl ligands, that of the hydrotris(pyrazolyl) borate (Tp) analogs is much less explored especially for noble metals, due to low accessibility to starting materials. We have recently reported the first reliable

route to synthesize rhodium thiolate complexes with Tp ancillary ligands and their chalcogenolate congeners [20,21]. The Rh(I) complex $[\text{TpRh}(\text{coe})(\text{MeCN})]$ ($\text{coe} = \eta^2\text{-cyclooctene}$) and its hydrotris(3,5-dimethylpyrazolyl)borate (Tp^*) analog $[\text{Tp}^*\text{Rh}(\text{coe})(\text{MeCN})]$ (**1**) [22] react with a range of organic disulfides to give mononuclear bis(thiolate) complexes, as exemplified in Eq. (1). Further conversion to dinuclear complexes bridged by μ -thiolate ligands has been also achieved. Here, we discuss the reactivities of bis(thiolate) complex **2** toward organic molecules and its application to catalytic C–S bond formation.



* Corresponding author. Fax: +81 3 5452 6362.

E-mail address: ymizobe@iis.u-tokyo.ac.jp (Y. Mizobe).

2. Results and discussion

2.1. Reactivities of $[\text{Tp}^*\text{Rh}(\text{SPh})_2(\text{MeCN})]$ toward organic molecules

The bis(thiolate) complex $[\text{Tp}^*\text{Rh}(\text{SPh})_2(\text{MeCN})]$ (**2**) [20] was treated with several organic molecules to examine the reactivity at the metal center. When **2** was treated with excess XyNC at room temperature, the MeCN ligand in **2** was smoothly replaced by XyNC to form $[\text{Tp}^*\text{Rh}(\text{SPh})_2(\text{XyNC})]$ (**3**). Complex **3** has been characterized by spectroscopic methods and unambiguously by X-ray diffraction study as shown in Fig. 1 and Table 1. The Rh center of **3** adopts a slightly distorted octahedral geometry as observed for **2**, whose structure has been previously confirmed by the X-ray analysis of the *p*-toluenethiolate analog $[\text{Tp}^*\text{Rh}(\text{SC}_6\text{H}_4\text{Me-}p)_2(\text{MeCN})]$ (**2'**) [20]. Three Rh–N bond distances in **3** are almost the same, indicating that the *trans* influence of XyNC ligand is comparable to that of benzenethiolate. The Rh–N bond at the *trans* position of XyNC in **3** at 2.132(2) Å is much longer than that *trans* to MeCN at 2.056(3) Å in **2'**, while the other corresponding Rh–S and Rh–N distances are not significantly different between **3** and **2'**. Linear structure of the Rh–C–N–Xy linkage and the $\text{C}\equiv\text{N}$ stretching frequency are in good agreement with those of $[\text{Tp}^*\text{Rh}(\eta^2\text{-S}_5)(\text{XyNC})]$ ($\nu_{\text{N}\equiv\text{C}}$ at 2187 cm^{-1}) [23].

Although **2** showed no reactivity toward alkenes, it smoothly reacted with various terminal alkynes $\text{RC}\equiv\text{CH}$ (R = alkyl, aryl) at ambient temperature to yield the rhodathiacyclobutene complexes $[\text{Tp}^*\text{Rh}(\text{SPh})\{\eta^2\text{-CH}=\text{CR}(\text{SPh})\}]$ (**4**) (Eq. (2)). Thermal instability (vide infra) and high solubility in common organic solvents prevented isolation of most of **4** except for **4a** (R = CH_2Ph) and **4b** (R = Ph). The molecular structure of **4a** was fully

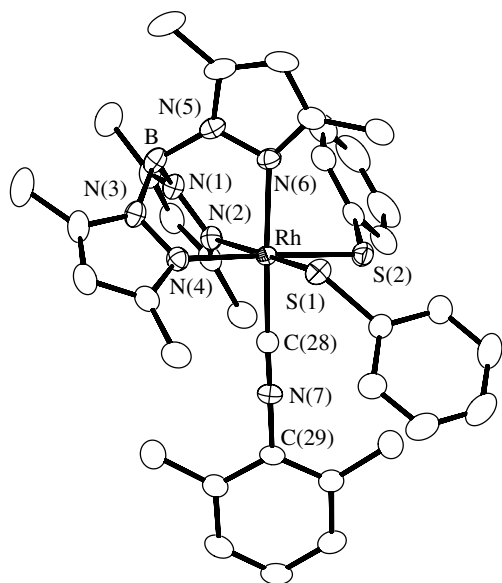


Fig. 1. Molecular structure of **3**. Hydrogen atoms are omitted for clarity.

Table 1
Selected bonding parameters in **3**

Bond lengths (Å)			
Rh–S(1)	2.3574(6)	Rh–S(2)	2.3534(5)
Rh–N(2)	2.124(2)	Rh–N(4)	2.138(2)
Rh–N(6)	2.132(2)	Rh–C(28)	1.902(2)
S(1)–C(16)	1.776(2)	S(2)–C(22)	1.775(2)
N(7)–C(28)	1.149(3)	N(7)–C(29)	1.397(3)
Bond angles (°)			
S(1)–Rh–S(2)	91.80(2)	S(1)–Rh–N(2)	173.88(4)
S(1)–Rh–C(28)	90.25(7)	S(2)–Rh–N(4)	177.93(5)
S(2)–Rh–C(28)	84.96(6)	N(6)–Rh–C(28)	177.51(9)
Rh–C(28)–N(7)	177.1(2)	C(28)–N(7)–C(29)	174.2(2)

determined by X-ray crystallography, as shown in Fig. 2 and Table 2. The planar 4-membered ring consists of the Rh–S and alkyne moiety, with terminal C atom bound to Rh. The Rh–C(28) and the C(28)–C(29) distances are typical of the Rh–C single and C–C double bonds, respectively. Hydrogen atom attached to C(28) have been found in difference Fourier map, and sum of the bond angles around C(28) at 359° as well as that around C(29) at 360° indicate planar geometry of the rhodathiacyclobutene moiety. Two Rh–S distances are almost comparable, while *trans* influence of thioether unit is weaker than that of thiolate ligand as reflected in the Rh–N(2) and Rh–N(4) distances at 2.076(3) and 2.159(4) Å, respectively. Configuration of the phenyl group bound to S(1) is *anti* to the thiolate ligand (I in Eq. (3)). Distorted structure of the rhodathiacyclobutene ring is quite similar to the 4-membered ring in $[\text{Tp}^*\text{Rh}(\eta^2\text{-S-2-C}_5\text{H}_4\text{N})(\eta^1\text{-S-2-C}_5\text{H}_4\text{N})]$ [20].

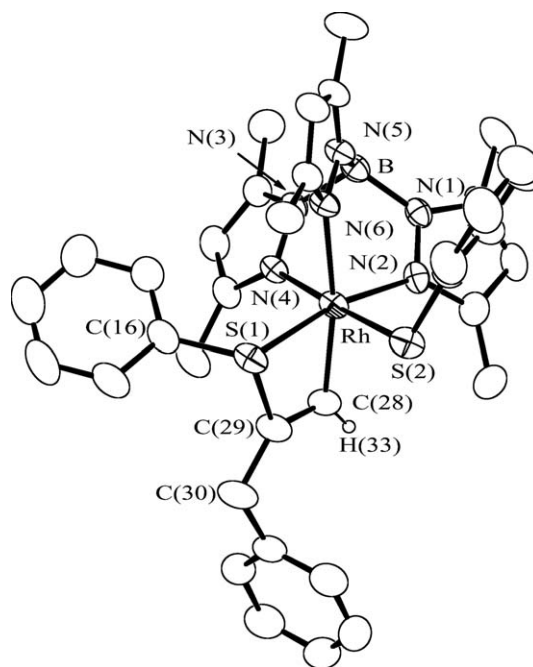
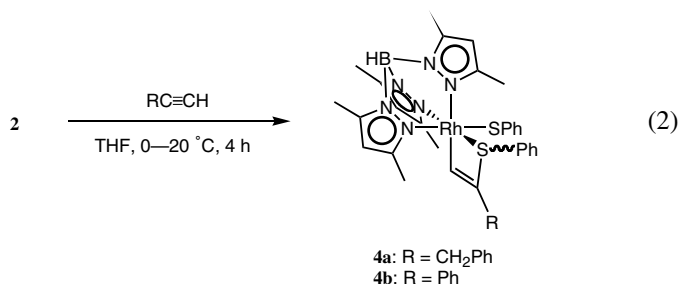


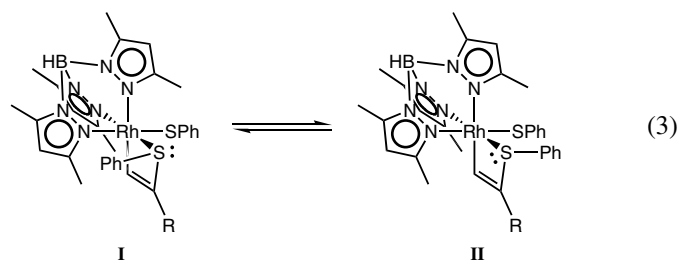
Fig. 2. Molecular structure of **4a**. Hydrogen atoms except for H(33) are omitted for clarity.

Table 2
Selected bonding parameters in **4a**

Bond lengths (Å)			
Rh–S(1)	2.341(1)	Rh–S(2)	2.345(2)
Rh–N(2)	2.076(3)	Rh–N(4)	2.159(4)
Rh–N(6)	2.150(3)	Rh–C(28)	1.994(4)
S(1)–C(16)	1.789(6)	S(1)–C(29)	1.819(4)
S(2)–C(22)	1.775(5)	C(28)–C(29)	1.326(6)
C(29)–C(30)	1.504(7)	C(28)–H(33)	0.86(3)
Bond angles (°)			
S(1)–Rh–S(2)	81.77(5)	S(1)–Rh–N(2)	168.0(1)
S(1)–Rh–C(28)	69.5(1)	S(2)–Rh–N(4)	174.99(8)
S(2)–Rh–C(28)	86.2(2)	N(6)–Rh–C(28)	168.3(1)
Rh–S(1)–C(16)	115.4(1)	Rh–S(1)–C(29)	79.8(1)
C(16)–S(1)–C(29)	106.9(2)	Rh–C(28)–C(29)	107.0(3)
Rh–C(28)–H(33)	130(2)	C(29)–C(28)–H(33)	122(2)
S(1)–C(29)–C(28)	103.5(3)	S(1)–C(29)–C(30)	119.9(3)
C(28)–C(29)–C(30)	136.6(4)		



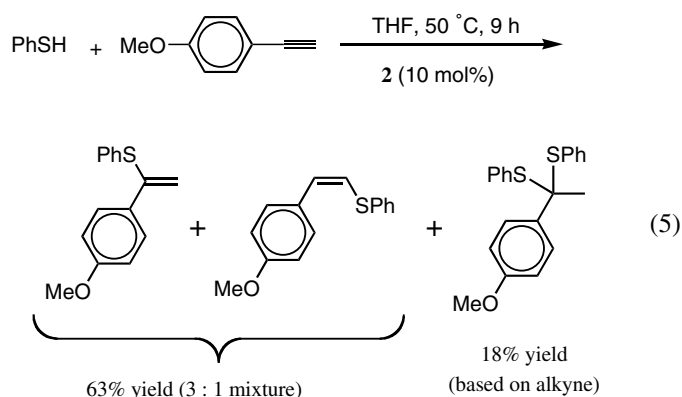
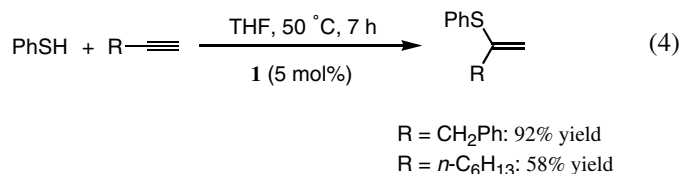
In contrast to the crystal structure of **4a**, each ¹H NMR spectrum of **4** indicates the existence of two species in solution. Chemical shifts of hydrogen atom directly attached to the rhodathiacyclobutene ring of both species are close, and they are coupled with Rh atom of comparable coupling constants. Three pyrazolyl moieties in each species are inequivalently observed as expected. Therefore, it is concluded that those species differ in configuration with respect to the phenyl group bound to the metallacycle and are in equilibrium in solution (Eq. (3)).



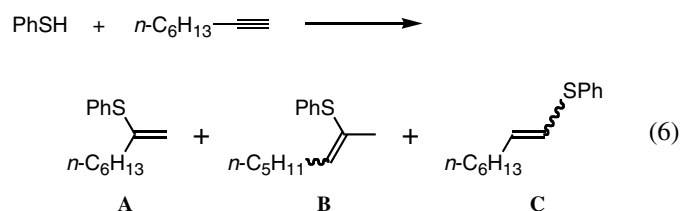
2.2. Catalytic addition of benzenethiol to terminal alkynes

Complex **4** was found to be unstable even at room temperature. Its decomposition formed uncharacterized Rh species and R(PhS)C=CH₂. Since these vinyl thioethers are presumed to be generated by protonation of η²-CH=CR(SPh) ligands, addition reactions of PhSH to RC≡CH have been examined, and it has been found that **2** as well as **1** promote these reactions catalytically. Thus, in the presence of 5 mol%

of **1**, reactions of 3-phenylpropyne or 1-octyne with equimolar amount of PhSH proceeded regioselectively at 50 °C to afford the Markovnikov products, which were isolated in 92% or 58% yields, respectively (Eq. (4)). However, **1** was not so effective for the reaction of *p*-MeOC₆H₄C≡CH with PhSH. On the other hand, **2** could catalyze even the hydrothiolation of *p*-MeOC₆H₄C≡CH, although larger amount of catalyst (10 mol%) and longer reaction time were necessary for completion and concomitant formations of the regioisomer *cis-p*-MeOC₆H₄CH=CHSPh and the thioketal *p*-MeOC₆H₄C(SPh)₂CH₃ were observed (Eq. (5)).



Vinyl thioethers are significant intermediates for synthesizing important organosulfur compounds, and metal-catalyzed hydrothiolation of non-activated alkynes leading to them has been preceded. Some noble metal complexes have been reported to be active, whose product selectivities are compared as follows by referring the reaction of 1-octyne and PhSH as representative (Eq. (6)). Thus, reactions using Pd(CH₃CO₂)₂ [24] or combination of [Ni(PMePh₂)₄] and Ph₂P(O)OH [25] are known to afford the isomer **A**, similarly to our result. In contrast, migration of double bond leading to **B** occurs in the catalysis by [PdCl₂(PhCN)₂] or [Pt(PPh₃)₄], while the use of [RhCl(PPh₃)₃] in EtOH has been found to provide the regioisomer *trans*-**C** [24,26].

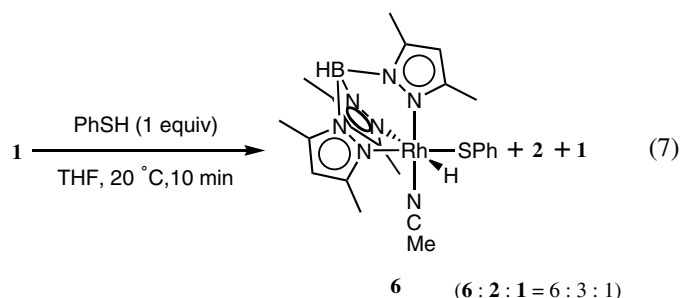


Several Rh(I) and Ir(I) complexes having bidentate N-donor co-ligands have also been shown to promote hydrothiolation [27]. Very recently, Love and coworkers have reported that $[\text{Tp}^*\text{Rh}(\text{PPh}_3)_2]$ (**5**) is an active catalyst, especially for addition of alkanethiols [28]. Most reactions of $\text{R}'\text{SH}$ and $\text{RC}\equiv\text{CH}$ using **5** provide the branched isomer $\text{R}(\text{R}'\text{S})\text{C}=\text{CH}_2$ exclusively, exhibiting the regioselectivity similar to the systems using **1** and **2**, while **5** considerably causes migration of double bond if $\text{R} = \text{primary alkyl}$ (forming analog of **B** in Eq. (6)). Both **5** and **2** show modest regioselectivity in the reaction between PhSH and arylacetylenes to afford the same branched isomer as the major product. However, geometries of the minor linear isomers make a sharp contrast, as *trans-p*- $\text{MeOC}_6\text{H}_4\text{CH}=\text{CHSPh}$ was formed by **5** and *cis-p*- $\text{MeOC}_6\text{H}_4\text{CH}=\text{CHSPh}$ by **2**.

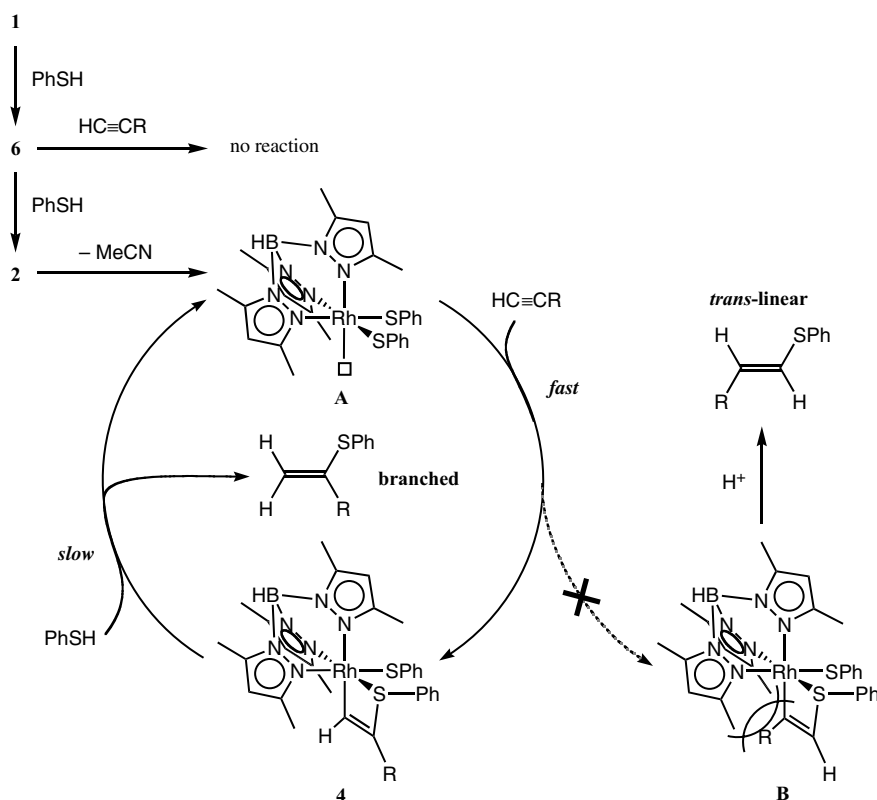
2.3. Mechanistic study of the catalysis

When **1** was treated with an equimolar amount of PhSH , the hydride–thiolate complex $[\text{Tp}^*\text{RhH}(\text{SPh})(\text{MeCN})]$ (**6**) was predominantly formed via oxidative addition of PhSH together with bis(thiolate) complex **2** and unreacted **1** (Eq. (7)) [29]. Treatment of **1** with excess PhSH afforded **2** in higher yield with concomitant formation of H_2 . ^1H NMR spectrum of **6** in C_6D_6 shows a hydrido signal at $\delta -13.79$, which is coupled with a Rh atom at 11.6 Hz. Three pyrazolyl groups are observed inequivalently, and a singlet for one MeCN ligand appears at $\delta 0.36$. In contrast to **2**, **6** showed

no reactivity toward terminal alkynes at ambient temperature. These findings indicate that the active species is also **2** in the reaction using **1** as the catalyst precursor, if **1** initially reacts with PhSH . It is to be noted that several Tp-Rh(I) complexes having alkene ligands are reported to catalyze polymerization of arylacetylenes but not to interact with alkylacetylenes [30]. In addition, $[\text{Tp}^*\text{Rh}(\text{PR}_3)_2]$ ($\text{R} = \text{Ph}$, $\text{C}_6\text{H}_4\text{F-p}$) has been known to react with phenylacetylene to give $[\text{Tp}^*\text{RhH}(\text{C}\equiv\text{CPh})(\text{PR}_3)]$ [31]. Therefore, the reactivity of arylacetylenes toward **1** is estimated to be higher than that of less acidic alkylacetylenes, and the substantial reaction with alkyne prior to PhSH may result in less effectiveness of **1** than **2** as observed in the reaction with *p*- $\text{MeOC}_6\text{H}_4\text{C}\equiv\text{CH}$.



It is most probable that the catalytic cycle to afford the branched product $\text{R}(\text{PhS})\text{C}=\text{CH}_2$ proceeds according to the cycle depicted in Scheme 1. Coordinatively unsaturated



species **A** generated by dissociation of MeCN from **2** reacts regioselectively with $\text{RC}\equiv\text{CH}$ to form **4**, whose protonation by PhSH followed by coordination of the resulting PhS^- and liberation of the product regenerate **A**. Alkylacetylenes are considered to react in such a simple manner, exhibiting high selectivity, but other reaction pathways may exist in less selective reactions of arylacetylenes. If C–S bond formation occurs at the terminal side of $\text{RC}\equiv\text{CH}$ in a certain ratio, it may lead to **B**, in which R group will heavily congest with dimethylpyrazolyl moieties in Tp^* . In fact, the protonation product of **B**, *trans*- $\text{RCH}=\text{CHSPh}$, could not be detected, neglecting the path to **B**.

To clarify detailed mechanism, the reactions of PhSH and *p*- $\text{MeOC}_6\text{H}_4\text{C}\equiv\text{CH}$ using **2** under various conditions were monitored by NMR spectroscopy. Typical time course of the reaction is shown in Fig. 3, where the increase of two products, the branched isomer *p*- $\text{MeOC}_6\text{H}_4(\text{PhS})\text{C}=\text{CH}_2$ and the *cis*-linear *cis*-*p*- $\text{MeOC}_6\text{H}_4\text{CH}=\text{CHSPh}$, corresponds well to the consumption of the substrate. As indicated in Figs. 4 and 5, high concentration of **2** or PhSH increased the rate of the branched isomer production, while that of alkyne was proved to show no influence essentially (Fig. 6). These observations suggest that the rate determining step of the catalytic cycle is the interaction of **4** with PhSH to liberate the branched isomer, and that the reaction of **A** with alkyne to form **4** is quite a fast step. On the other hand, formation of the *cis*-linear isomer was highly dependent on concentration of alkyne (Fig. 6) but not affected by **2** or PhSH. Therefore, it is concluded that the linear isomer have independently been formed via nucleophilic [32,33] or radical [27,34] mechanisms. Formation of the thioketal *p*- $\text{MeOC}_6\text{H}_4\text{C}(\text{SPh})_2\text{CH}_3$ is also rationalized by Markovnikov addition of PhSH to *p*- $\text{MeOC}_6\text{H}_4(\text{PhS})\text{C}=\text{CH}_2$.

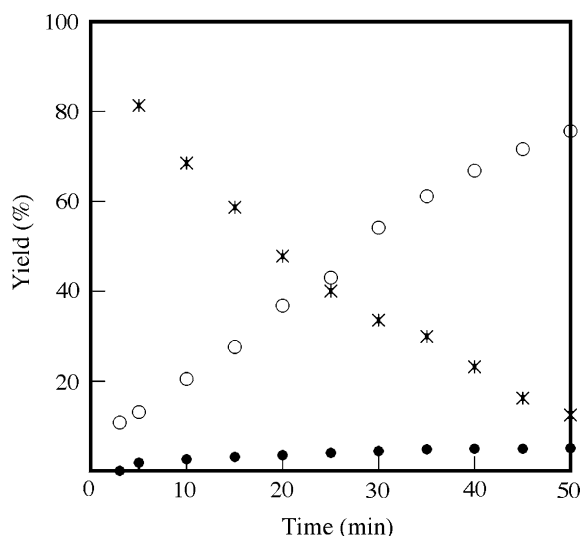


Fig. 3. Time course of the reaction of PhSH and *p*- $\text{MeOC}_6\text{H}_4\text{C}\equiv\text{CH}$ catalyzed by **2** in C_6D_6 at 50°C . Initial conditions: $[\text{PhSH}]_0 = [\text{p-MeOC}_6\text{H}_4\text{C}\equiv\text{CH}]_0 = 70 \text{ mmol L}^{-1}$, $[\mathbf{2}] = 10 \text{ mmol L}^{-1}$. Open and filled circles represents the yields of *p*- $\text{MeOC}_6\text{H}_4(\text{PhS})\text{C}=\text{CH}_2$ and *cis*-*p*- $\text{MeOC}_6\text{H}_4\text{CH}=\text{CHSPh}$, respectively, and * denotes the percentage quantity of *p*- $\text{MeOC}_6\text{H}_4\text{C}\equiv\text{CH}$ ($100 \times [\text{p-MeOC}_6\text{H}_4\text{C}\equiv\text{CH}] / [\text{p-MeOC}_6\text{H}_4\text{C}\equiv\text{CH}]_0$).

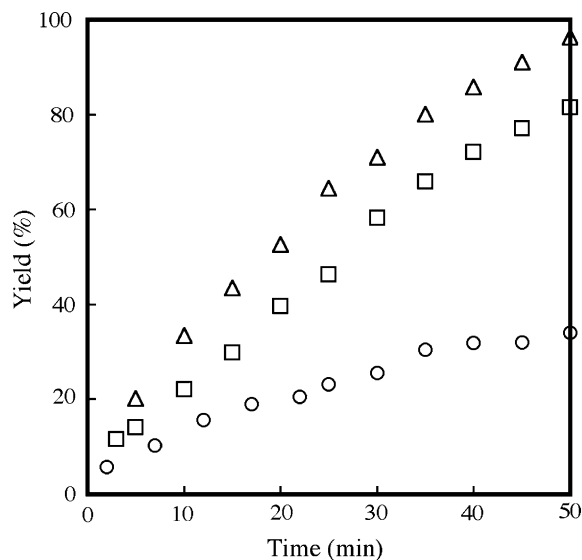


Fig. 4. Time course of the yield of *p*- $\text{MeOC}_6\text{H}_4(\text{PhS})\text{C}=\text{CH}_2$ under different catalyst concentrations. Initial conditions: $[\text{PhSH}]_0 = [\text{p-MeOC}_6\text{H}_4\text{C}\equiv\text{CH}]_0 = 70 \text{ mmol L}^{-1}$ (all), $[\mathbf{2}] = 5$ (circle), 10 (square), 15 (triangle) mmol L^{-1} .

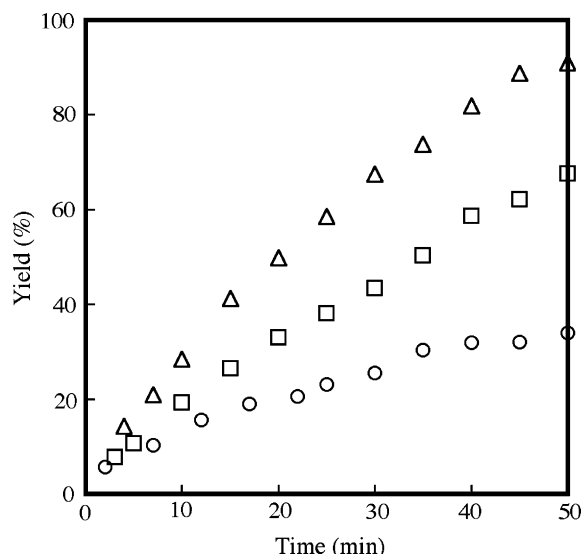


Fig. 5. Time course of the yield of *p*- $\text{MeOC}_6\text{H}_4(\text{PhS})\text{C}=\text{CH}_2$ with different amounts of PhSH. Initial conditions: $[\text{p-MeOC}_6\text{H}_4\text{C}\equiv\text{CH}]_0 = 70 \text{ mmol L}^{-1}$, $[\mathbf{2}] = 5 \text{ mmol L}^{-1}$ (all), $[\text{PhSH}]_0 = 70$ (circle), 140 (square), 210 (triangle) mmol L^{-1} .

In summary, Tp-Rh complexes **1** and **2** have been found to catalyze addition reaction of PhSH to alkylacetylenes with high activity and excellent selectivity, where the key intermediate involved in the catalytic cycle has been fully characterized.

3. Experimental

All manipulations were performed under nitrogen atmosphere using standard Schlenk techniques. Solvents were dried by common procedures and distilled under nitrogen before use. Complexes **1** [22] and **2** [20] were prepared

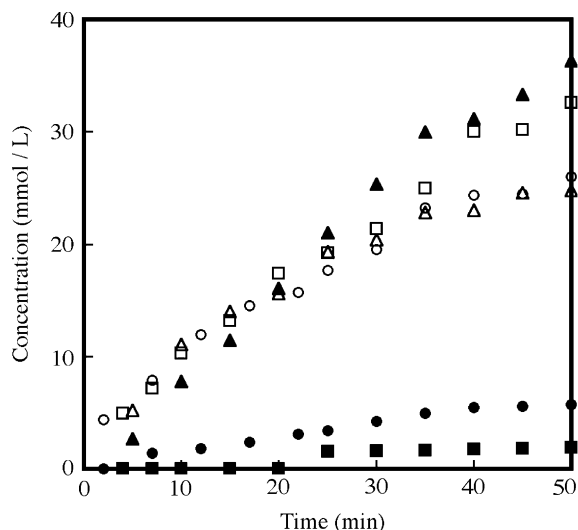


Fig. 6. Formation of *p*-MeOC₆H₄(PhS)C=CH₂ (open marks) and *cis-p*-MeOC₆H₄C=CHSPh (filled marks) with different amounts of alkyne. Initial conditions: [PhSH]₀ = 70 mmol L⁻¹, [2] = 5 mmol L⁻¹ (all), [*p*-MeOC₆H₄C≡CH]₀ = 35 (square), 70 (circle), 140 (triangle).

according to the literature methods. Other reagents were commercially available and used as received.

NMR spectra (¹H at 400 MHz and ¹³C at 100.5 MHz) were recorded on a JEOL alpha-400 spectrometer, and chemical shifts were referenced using those of residual solvent resonances (CDCl₃ at δ_H 7.26 and δ_C 77.00, and C₆D₆ at δ_H 7.15 ppm). IR spectra were recorded on a JASCO FT/IR-420 spectrometer. Elemental analyses were done with a Perkin–Elmer 2400 series II CHN analyzer.

3.1. Synthesis of [Tp*Rh(SPh)₂(XyNC)] (3)

A THF solution (5 mL) of **2** (68 mg, 0.10 mmol) and XyNC (28 mg, 0.21 mmol) was stirred at room temperature for 17 h. The resulting red solution was concentrated to 2 mL followed by addition of hexane (18 mL). Red crystals of **3** were filtered off and dried in vacuum (51 mg, 68% yield). Anal. Calc. for C₃₆H₄₁N₇BS₂Rh: C, 57.68; H, 5.51; N, 13.08. Found: C, 57.62; H, 5.55; N, 12.90%. ¹H NMR (C₆D₆): δ 2.12, 2.13 (s, 6H each, Me in Xy and Tp*), 2.21, 3.34 (s, 3H each, Me in Tp*), 2.49 (s, 6H, Me in Tp*), 5.48 (s, 2H, CH in Tp*), 5.56 (s, 1H, CH in Tp*), 6.52 (d, 2H, 3,5-H in Xy), 6.54 (t, 1H, 4-H in Xy), 6.6–7.2 (m, 10H, Ph). IR (KBr): 2527 (ν_{B-H}), 2192 (ν_{N=C}) cm⁻¹.

3.2. Synthesis of [Tp*Rh(SPh){η²-CH=C(CH₂Ph)-(SPh)}] (4a)

To a THF solution (5 mL) of **2** (66 mg, 0.10 mmol) was added PhCH₂C≡CH (19 μL, 0.15 mmol) at 0 °C. After stirring the mixture for 4 h at 0 °C, the resulting purple solution was concentrated to 2 mL. After addition of hexane (18 mL), the mixture was stored at -20 °C, yielding purple crystals of **4a** · 0.5THF (20 mg, 26% yield). Anal. Calc. for C₃₈H₄₄O_{0.5}N₆BS₂Rh: C, 59.22; H, 5.75; N,

10.91. Found: C, 58.95; H, 5.89; N, 11.29%. ¹H NMR (C₆D₆): δ (major isomer) 1.63, 2.21, 2.22, 2.30, 2.41, 2.74 (s, 3H each, Me in Tp*), 3.6–3.75 (m, 2H, CH₂), 5.40, 5.44, 5.61 (s, 1H each, CH in Tp*), 6.5–7.8 (m, 15H, Ph), 8.59 (dt, *J*_{Rh-H} = 3.2, *J*_{H-H} = 1.2 Hz, 1H, RhCH), (minor isomer) 1.94, 2.14, 2.17, 2.30, 2.33, 2.61 (s, 3H each, Me in Tp*), 3.27, 3.58 (dd, *J*_{H-H} = 16, 1.2 Hz, 1H each, CH₂), 5.31, 5.49, 5.53 (s, 1H each, CH in Tp*), 6.5–7.8 (m, 15H, Ph), 8.73 (dt, *J*_{Rh-H} = 3.0, *J*_{H-H} = 1.2 Hz, 1H, RhCH), major:minor = 1:0.9, ca. 0.5 molar amount of THF (δ 1.40 and 3.57) was detected. IR (KBr): 2520 (ν_{B-H}) cm⁻¹.

3.3. Synthesis of [Tp*Rh(SPh){η²-CH=CPh(SPh)}] (4b)

Reaction of **2** (66 mg, 0.10 mmol) and PhC≡CH (17 μL, 0.15 mmol) was carried out according to the above method for **4a**. Extraction with ether followed by concentration and standing at -20 °C gave purple crystals of **4b** · 0.25(Et₂O) (31 mg, 42% yield). Anal. Calc. for C₃₆H_{40.5}N₆O_{0.25}BS₂Rh: C, 58.50; H, 5.52; N, 11.37. Found: C, 57.95; H, 5.54; N, 10.98%. ¹H NMR (C₆D₆): δ (major isomer) 2.03, 2.14, 2.21, 2.33, 2.44, 2.82 (s, 3H each, Me in Tp*), 5.44, 5.45, 5.59 (s, 1H each, CH in Tp*), 6.3–7.7 (m, 15H, Ph), 9.82 (d, *J*_{Rh-H} = 3.2 Hz, 1H, RhCH), (minor isomer) 1.63, 2.19, 2.20, 2.32, 2.72, 2.83 (s, 3H each, Me in Tp*), 5.34, 5.51, 5.69 (s, 1H each, CH in Tp*), 6.3–7.7 (m, 15H, Ph), 9.57 (d, *J*_{Rh-H} = 3.6 Hz, 1H, RhCH), major:minor = 1:0.5, ca. 0.25 molar amount of Et₂O (δ 1.11 and 3.25) was detected. IR (KBr): 2526 (ν_{B-H}) cm⁻¹.

3.4. Catalytic addition of PhSH to RCH₂CCH by using 1

To a solution of **1** (14 mg, 0.025 mmol) in THF (3 mL) were added PhCH₂C≡CH (63 mg, 0.54 mmol) and PhSH (61 mg, 0.55 mmol) at 0 °C, and the mixture was stirred at 50 °C for 7 h. After evaporation of volatiles under vacuum at room temperature, the residual oil was purified by column chromatography on silica gel using hexane–ether as eluent to provide PhCH₂(PhS)C=CH₂ (112 mg, 92%). Anal. Calc. for C₁₅H₁₄S: C, 79.60; H, 6.23. Found: C, 79.74; H, 6.35%. ¹H NMR (CDCl₃): δ 3.53 (br s, 2H, CH₂Ph), 5.00 (s, 1H, =CH₂), 5.12 (t, *J* = 1.2 Hz, 1H, =CH₂), 7.2–7.5 (m, 10H, Ph). ¹³C{¹H} NMR (CDCl₃): δ 42.95 (CH₂Ph), 114.65 (=CH₂), 126.62, 127.99, 128.43, 129.12, 129, 21, 133.01, 133.41, 138.44 (Ph), 145.22 (C=CH₂).

Reaction of PhSH (58 mg, 0.52 mmol) and *n*-C₆H₁₃C≡CH (56 mg, 0.51 mmol) in a similar procedure followed by chromatography (silica gel, hexane as eluent) afforded *n*-C₆H₁₃(PhS)C=CH₂ (65 mg, 58% yield). ¹H NMR (CDCl₃): δ 0.88 (t, *J* = 6.8 Hz, 3H, CH₃), 1.2–1.35 (m, 6H, CH₂), 1.5–1.6 (m, 2H, CH₂), 2.23 (t, *J* = 7.2 Hz, 2H, CH₂C=), 4.86, 5.14 (s, 1H each, =CH₂), 7.25–7.45 (m, 5H, Ph). ¹³C{¹H} NMR (CDCl₃): δ 14.16 (CH₃), 22.64, 28.43, 28.63, 31.64, 36.59 ((CH₂)₅), 112.38 (=CH₂), 127.62, 128.99, 133.12, 133.15 (Ph), 146.04 (C=CH₂).

3.5. Catalytic addition of PhSH to *p*-MeOC₆H₄CCH by using **2**

A THF solution (3 mL) of PhSH (55 mg, 0.50 mmol), *p*-MeOC₆H₄C≡CH (66 mg, 0.50 mmol), and **2** (33 mg, 0.050 mmol) was stirred at 50 °C for 9 h. Volatiles were evaporated under vacuum at room temperature, and the residue was chromatographed on silica gel with hexane–toluene to provide a 3:1 mixture (76 mg, 63% yield) of *p*-MeOC₆H₄(PhS)C=CH₂ and *cis*-*p*-MeOC₆H₄CH=CHSPh as the first fraction and *p*-MeOC₆H₄C(SPh)₂CH₃ (32 mg, 18% yield based on alkyne) as the second. Mixture of *p*-MeOC₆H₄(PhS)C=CH₂ and *cis*-*p*-MeOC₆H₄CH=CHSPh: Anal. Calc. for C₁₅H₁₄OS: C, 74.34; H, 5.82. Found: C, 74.42; H, 5.41%. *p*-MeOC₆H₄(PhS)C=CH₂: ¹H NMR (CDCl₃): δ 3.78 (s, 3H, OMe), 5.24, 5.59 (s, 1H each, =CH₂), 6.82, 7.55 (d, *J* = 8.8 Hz, 2H each, C₆H₄), 7.15–7.45 (m, 5H, Ph). ¹³C{¹H} NMR (CDCl₃): δ 55.26 (OMe), 114.68 (=CH₂), 143.55 (C=CH₂), 113.55, 127.03, 128.32, 128.91, 131.07, 131.55, 134.03, 159.68 (aromatic). *cis*-*p*-MeOC₆H₄CH=CHSPh: ¹H NMR (CDCl₃): δ 3.83 (s, 3H, OMe), 6.37, 6.56 (d, *J* = 10.8 Hz, 1H each, CH=CH), 6.93, 7.49 (d, *J* = 8.8 Hz, 2H each, C₆H₄), 7.1–7.5 (m, 5H, Ph). ¹³C{¹H} NMR (CDCl₃): δ 55.30 (OMe), 123.15, 127.11 (CH=CH), 113.65, 126.92, 129.03, 129.20, 129.77, 130.07, 136.31, 158.52 (aromatic). *p*-MeOC₆H₄C(SPh)₂CH₃: Anal. Calc. for C₁₅H₁₄OS: C, 71.55; H, 5.72. Found: C, 71.75; H, 5.66%. ¹H NMR (CDCl₃): δ 1.80 (s, 3H, CMe), 3.82 (s, OMe), 6.81, 7.51 (d, *J* = 9.0 Hz, 2H each, C₆H₄), 7.2–7.35 (m, 10H, Ph). ¹³C{¹H} NMR (CDCl₃): δ .27.75 (CMe), 55.30 (OMe), 63.56 (CMe), 113.08, 128.31, 128.76, 128.78, 132.59, 135.39, 136.24, 158.61 (aromatic).

3.6. Reaction of **1** with PhSH

To a THF solution (5 mL) of **1** (62 mg, 0.11 mmol) was added PhSH (12 mg, 0.11 mmol), and the mixture was stirred at 20 °C for 10 min. NMR measurement of the resulting solution revealed existence of [Tp*⁺RhH(SPh)(MeCN)] (**6**), **2**, and **1** in a 6:3:1 ratio. After addition of *p*-MeOC₆H₄C≡CH (14 mg, 0.11 mmol) to the solution and standing for 10 min, signals of **1** and **2** disappeared while those of **6** remained unchanged. ¹H NMR (C₆D₆): δ -13.79 (d, *J*_{Rh-H} = 11.6 Hz, 1H, RhH), 0.36 (s, 3H, MeCN), 2.07, 2.15, 2.31, 2.32, 2.72, 2.84 (s, 3H each, Me in Tp*), 5.42, 5.64, 5.86 (s, 1H each, CH in Tp*), 6.94 (br t, *J*_{H-H} ~ 7.4 Hz, 2H, *m*-H in Ph), 8.15 (dd, *J*_{H-H} = 8.4, 1.2 Hz, 2H, *o*-H in Ph), signal of *p*-H in Ph is overlapping with that of C₆HD₅.

3.7. Crystallographic study

Single crystals of **3** and **4a** · 0.5THF were sealed in glass capillaries under argon and mounted on a Rigaku Mercury-CCD diffractometer equipped with a graphite mono-

Table 3
Crystallographic data for **3** and **4a** · 0.5THF

	3	4a · 0.5THF
Formula	C ₃₆ H ₄₁ BN ₇ S ₂ Rh	C ₃₈ H ₄₄ BN ₆ O _{0.5} S ₂ Rh
Formula weight	749.60	770.64
Space group	<i>P</i> 2 ₁ / <i>c</i> (#14)	<i>P</i> 1̄ (#2)
<i>a</i> (Å)	11.004(1)	12.004(5)
<i>b</i> (Å)	18.056(2)	13.019(4)
<i>c</i> (Å)	18.707(2)	13.593(5)
α (°)	90	67.48(2)
β (°)	103.2432(5)	85.81(2)
γ (°)	90	71.28(2)
<i>V</i> (Å ³)	3617.9(8)	1855(1)
<i>Z</i>	4	2
<i>d</i> _{calcd} (g Å ⁻³)	1.376	1.379
μ (mm ⁻¹)	0.622	0.609
Number of unique reflections (<i>R</i> _{int})	8126 (0.019)	8142 (0.023)
Number of reflections <i>F</i> _o ² > 2σ(<i>F</i> _o ²)	6525	5336
Number of variables	468	474
<i>R</i> ₁ ^a (<i>F</i> _o ² > 2σ(<i>F</i> _o ²))	0.031	0.048
<i>wR</i> ₂ ^b (all data)	0.096	0.143
Goodness-of-fit ^c	1.018	1.018
Maximum/minimum <i>e</i> ⁻ density	1.18/−0.45	1.25/−0.88

$$^a R_1 = \sum ||F_o| - |F_c|| / \sum |F_o|.$$

$$^b wR_2 = [\sum w(F_o^2 - F_c^2)^2 / \sum w(F_o^2)^2]^{1/2}.$$

$$^c \text{Goodness-of-fit} = [\sum w(F_o^2 - F_c^2)^2 / \{(\text{no. unique}) - (\text{no. variables})\}]^{1/2}.$$

chromatized Mo Kα source. All diffraction studies were done at 23 °C, whose details are listed in Table 3.

Structure solution and refinements were carried out by using the CRYSTALSTRUCTURE program package [35]. The positions of the non-hydrogen atoms were determined by Patterson methods (PATTY [36]) and subsequent Fourier synthesis (DIRDIF99 [37]), and they were refined with anisotropic thermal parameters by full-matrix least-squares techniques. The THF molecule in **4a** · 0.5THF disordered around the inversion center was refined isotropically with 0.5 atom occupancies and restraints. Hydrogen atoms bound to B atom and those bound to C(28) and C(30) in **4a** · 0.5THF were found in the Fourier maps and isotropically refined, while the other hydrogens were placed at the calculated positions. Refinements were done by using all unique data within the limits of 6.2° < 2θ < 55°.

Acknowledgements

This work was supported by a Grant-in-Aid for Scientific Research on Priority Areas (No. 14078206, “Reaction Control of Dynamic Complexes”) from the Ministry of Education, Culture, Sports, Science and Technology, Japan and by CREST of JST (Japan Science and Technology Agency). We also thank Ms. Chihiro S. Mochizuki of Kogakuin University for elemental analysis.

Appendix A. Supplementary material

Crystallographic data for the structural analysis have been deposited with the Cambridge Crystallographic Data

Centre, CCDC Nos. 294096 and 294097 for compounds **3** and **4a** · 0.5THF. Copies of this information obtained free of charge from The Director, CCDC, 12 Union Road, Cambridge CB2 1EZ, UK (fax: +44 1223 336 033, or e-mail: deposit@ccdc.cam.ac.uk or www: <http://www.ccdc.cam.ac.uk>). Supplementary data associated with this article can be found, in the online version, at doi:10.1016/j.jorganchem.2006.03.005.

References

- [1] E.I. Stiefel, K. Matsumoto (Eds.), Transition Metal Sulfur Chemistry, ACS Symposium Series 653, 1996.
- [2] D.W. Stephan, T.T. Nadasdi, Coord. Chem. Rev. 147 (1996) 147.
- [3] M. Hidai, Y. Mizobe, H. Matsuzaka, J. Organomet. Chem. 473 (1994) 1.
- [4] J.R. Dilworth, J. Hu, Adv. Inorg. Chem. 40 (1994) 411.
- [5] B. Krebs, G. Henkel, Angew. Chem., Int. Ed. Engl. 30 (1991) 769.
- [6] A. Nakamura, N. Ueyama, K. Tatsumi, Pure Appl. Chem. 62 (1990) 1011.
- [7] I.G. Dance, Polyhedron 5 (1986) 1037.
- [8] J.C. Bayón, C. Claver, A.M. Masdeu-Bultó, Coord. Chem. Rev. 193–195 (1999) 73.
- [9] (a) Y. Inada, Y. Nishibayashi, S. Uemura, Angew. Chem. Int. Ed. 44 (2005) 7715;
(b) S.C. Ammal, N. Yoshikai, Y. Inada, Y. Nishibayashi, E. Nakamura, J. Am. Chem. Soc. 127 (2005) 9428, and references therein.
- [10] (a) H. Matsuzaka, Y. Takagi, M. Hidai, Organometallics 13 (1994) 13;
(b) H. Shimada, J.-P. Qu, H. Matsuzaka, Y. Ishii, M. Hidai, Chem. Lett. 24 (1995) 671;
(c) J.-P. Qü, D. Masui, Y. Ishii, M. Hidai, Chem. Lett. 27 (1998) 1003.
- [11] H. Gao, R.J. Angelici, Organometallics 17 (1998) 3063.
- [12] B. Gail, N.M. Kostic, Inorg. Chem. 37 (1998) 1021.
- [13] Y. Nakayama, T. Shibahara, H. Fukumoto, A. Nakamura, K. Mashima, Macromolecules 29 (1996) 8014.
- [14] (a) M. Nishio, H. Matsuzaka, Y. Mizobe, T. Tanase, M. Hidai, Organometallics 13 (1994) 4214;
(b) M. Nishio, H. Matsuzaka, Y. Mizobe, M. Hidai, Organometallics 15 (1996) 965;
(c) Y. Ishii, K. Ogio, M. Nishio, M. Retbøll, S. Kuwata, H. Matsuzaka, M. Hidai, J. Organomet. Chem. 599 (2000) 221.
- [15] U. Koelle, Chem. Rev. 98 (1998) 1313.
- [16] T. Kondo, T. Mitsudo, Chem. Rev. 100 (2000) 3205.
- [17] A. Ogawa, J. Organomet. Chem. 611 (2000) 463.
- [18] H. Kuniyasu, H. Kurosawa, Chem. Eur. J. 8 (2002) 2660.
- [19] F. Alonso, I.P. Beletskaya, M. Yus, Chem. Rev. 104 (2004) 3079.
- [20] H. Seino, T. Yoshikawa, M. Hidai, Y. Mizobe, Dalton Trans. (2004) 3593.
- [21] S. Nagao, H. Seino, M. Hidai, Y. Mizobe, Dalton Trans. (2005) 3166.
- [22] K. Ohta, M. Hashimoto, Y. Takahashi, S. Hikichi, M. Akita, Y. Moro-oka, Organometallics 18 (1999) 3234.
- [23] S. Nagao, N. Saito, A. Kojima, H. Seino, Y. Mizobe, Bull. Chem. Soc. Jpn. 78 (2005) 1641.
- [24] H. Kuniyasu, A. Ogawa, K.-I. Sato, I. Ryu, N. Kambe, N. Sonoda, J. Am. Chem. Soc. 114 (1992) 5902.
- [25] L.-B. Han, C. Zhang, H. Yazawa, S. Shimada, J. Am. Chem. Soc. 126 (2004) 5080.
- [26] A. Ogawa, T. Ikeda, K. Kimura, T. Hirao, J. Am. Chem. Soc. 121 (1999) 5108.
- [27] S. Burling, L.D. Field, B.A. Messerle, K.Q. Vuong, P. Turner, Dalton Trans. (2003) 4181.
- [28] C. Cao, L.R. Fraser, J.A. Love, J. Am. Chem. Soc. 127 (2005) 17614.
- [29] In sharp contrast to this result, reaction of **5** with C₆F₅SH has been described to lead to dissociation and degradation of Tp* ligand to yield [(PPh₃)₂Rh(μ-SC₆F₅)₂RhH(SC₆F₅)(PPh₃)(3,5-Me₂C₃H₂N₂)]. V. Cîrcu, M.A. Fernandes, L. Carlton, Polyhedron 22 (2003) 3293.
- [30] H. Katayama, K. Yamamura, Y. Miyaki, F. Ozawa, Organometallics 16 (1997) 4497.
- [31] V. Cîrcu, M.A. Fernandes, L. Carlton, Inorg. Chem. 41 (2002) 3859.
- [32] W.E. Truce, G.J.W. Tichenor, J. Org. Chem. 37 (1972) 2391.
- [33] A. Kondoh, K. Takami, H. Yorimitsu, K. Oshima, J. Org. Chem. 70 (2005) 6468.
- [34] K. Griesbaum, Angew. Chem., Int. Ed. Engl. 9 (1970) 273.
- [35] CRYSTALSTRUCTURE 3.00: Crystal Structure Analysis Package, Rigaku and Rigaku/MS, 2000–2002. CRYSTALS Issue 10: D.J. Watkin, C.K. Prout, J.R. Carruthers, P.W. Betteridge, Chemical Crystallography Laboratory, Oxford, UK.
- [36] PATTY: P.T. Beurskens, G. Admiraal, G. Beurskens, W.P. Bosman, S. Garcia-Granda, R.O. Gould, J.M.M. Smits, C. Smykall, The DIRDIF Program System; Technical Report of the Crystallography Laboratory, University of Nijmegen, The Netherlands, 1992.
- [37] DIRDIF99: P.T. Beurskens, G. Admiraal, G. Beurskens, W.P. Bosman, R. de Gelder, R. Israel, J.M.M. Smits, The DIRDIF-99 Program System; Technical Report of the Crystallography Laboratory, University of Nijmegen, The Netherlands, 1999.